

Fluorescence Chemosensor for HSO_4^- Ion Based on Pyrrole-Substituted Salicylimine Zn^{2+} Complex: Nanomolar Detection

Umesh Fegade¹ · Jitendra Bhosale¹ · Hemant Sharma² ·
Narinder Singh² · Ratnamala Bendre¹ · Anil Kuwar¹

Received: 14 March 2015 / Accepted: 15 June 2015 / Published online: 3 July 2015
© Springer Science+Business Media New York 2015

Abstract A novel pyrrole-substituted salicylimine zinc (II) ion complex has been synthesized and evaluated its anion binding affinity. The probe **4** has high selectivity for HSO_4^- over other anions in $\text{CH}_3\text{OH}:\text{H}_2\text{O}$ (70:30, v/v) solvent system. The emission intensity of **4** was quenched upon addition of HSO_4^- . The probe **4** is highly selective for HSO_4^- with a detection limit of 40 nM. Photoinduced electron transfer (PET) is responsible for observed change. The binding affinity of **4** for HSO_4^- was further authenticated through ratiometric change in absorbance profile.

Keywords Pyrrole-substituted salicylimine · HSO_4^- · Ratiometric · Quenching

Introduction

Design of artificial receptors for investigating its discriminating binding or anions sensing properties has been interest for researcher in the field of supramolecular chemistry due to significant of anionic species in biology and environment

Electronic supplementary material The online version of this article (doi:10.1007/s10895-015-1599-9) contains supplementary material, which is available to authorized users.

✉ Ratnamala Bendre
bendres@rediffmail.com

✉ Anil Kuwar
kuwaras@gmail.com

¹ School of Chemical Sciences, North Maharashtra University, Jalgaon, MS 425001, India

² Department of Chemistry, Indian Institute of Technology, Ropar, Rupanagar, Punjab, India

[1–7]. Anion binding sites provided by synthetic receptors most commonly use positive charge, neutral or cationic hydrogen bond donors and/or Lewis acidic metal centres. There is cultivating proof to propose that convinced anion or, more particularly, anion-arene communications might be effectively developed in the design of synthetic receptors for anions [8–10]. Among the toxic anions acting as severe environmental pollutants and consequently having adverse health effects, in the middle of the entire range of oxo anions, the detection of HSO_4^- is an important as it is found in many agricultural fertilizers, industrial wastage, nuclear fuel waste and can have toxic consequences as a pollutant when it gets into the environment. Sensing of HSO_4^- from aqueous medium draws additional impetus as in most of the biological and environmental systems. It has several biological applications and generates toxic sulfate (SO_4^{2-}) ions at high pH, causing disease relating to skin, eyes and respiratory system [11–13].

Here, as part of our continue research in anion recognition study, we report a pyrrole-imines based zinc complex ‘turn-on’ chemosensor **4** for relatively beneath accepted sensing of HSO_4^- from aqueous medium. To the greatest of our awareness, the pyrrole-imine based zinc complex that have been reported so far are based on self-motivated quenching processes with no specific anion binding site and also there is little precedence of pyrrole-imine based sensors that are capable of binding and discriminating between the anions exhibiting static quenching processes. The functioning of sensor **4** for recognizing HSO_4^- is based on its appended pyrrole-imine Zn^{2+} complex functionality that acts as a binding as well as a ‘turn-off’ fluorescent sensing component. The anion binding sympathy of receptor **4** was evaluated by monitoring their respective UV-visible, fluorescence studies and DFT calculations have also been carried out to get information about the molecular site involved in recognizing and binding of the HSO_4^- anion. The sensors development has been suggested to

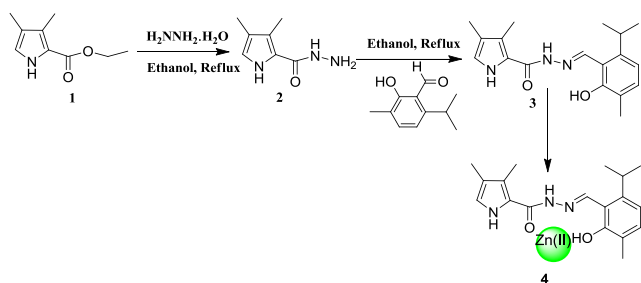
involve the hydrogen bonding between the HSO_4^- and pyrrole-imine linked of Zn^{2+} complex **4** affecting the photoactive behaviour of the pyrrole-imine moiety.

This involves the synthesis of fluorescent PET sensor designed for anion binding studies. Coordination sites in the receptor have one amide group and metal centre (Scheme 1). The binding ability of receptor **4** has been tested towards various anions (F^- , Cl^- , Br^- , I^- , HSO_4^- , NO_3^- , CH_3COO^- , and CN^-) in $\text{CH}_3\text{OH}:\text{H}_2\text{O}$ (70:30, v/v) solvent system and calculate the binding constant for anion (HSO_4^-) and which has shown distinct fluorescence recognition.

Result and Discussion

Scheme 1 shows the synthesis of the receptor and the zinc complex. The novel receptor was obtained by the Schiff bases were prepared by reaction of equimolar quantities of 3, 4-dimethyl-1*H*-pyrrole-2-carbohydrazide **2** and substituted aromatic aldehyde. Each reactant was dissolved in a minimum amount of ethanol, and then mixed together. The solution was refluxed for 3–4 h then cooled to room temperature and poured in to ice cold water (Scheme 1). The white compound **3** obtained was purified by recrystallization from ethanol and characterized by various spectroscopic techniques and Further complexation between the receptor **3** and the zinc chloride in methanol was carried out at room temperature. After 3 h, solid was precipitated, and then the precipitates were collected and washed with the small amount of cooled methanol. HR-MS measurement of an acetonitrile solution of the obtained residue showed peak at m/z 445.117, $[\text{Ligand} + \text{Zn}^{2+}] \cdot 2\text{Cl}^-$ corresponding to a mononuclear complex composed of Ligand/ $\text{Zn} = 1:1$. IR spectrum of the zinc complex indicated the structural information, in which the hydroxyl groups take part in the complexation with zinc since the band responsible for hydroxyl protons become broad and all data and spectra were reported in our previous paper [22]. Thus, the zinc complex has plenty of proton donating groups; which work in synergistic way to accommodate the anion.

Fluorescence and UV–vis studies were executed using a 10 μM of receptor **4** in a $\text{CH}_3\text{OH}:\text{H}_2\text{O}$ (70:30, v/v) solution with adding fixed amounts of anions solution. Solutions were



Scheme 1 Synthesis of receptor **4**

shaken for 30 min before measuring the absorption and fluorescence in order to make the anions with the sensors sufficiently. The colorimetric sensing abilities was precisely investigated by adding various anions (100 μM) such as F^- , Cl^- , Br^- , I^- , AcO^- , H_2PO_4^- , HSO_4^- and NO_2^- (tetrabutylammonium was used as a counteranion) to solution of receptor **4** (10 μM). When adding 10 equiv. of HSO_4^- to the $\text{CH}_3\text{OH}:\text{H}_2\text{O}$ (70:30, v/v) solution of receptor **4**, receptor **4** responded with dramatic colour changes from yellow green to colourless (Fig. 1 Inset). In the corresponding UV–vis spectrum, new and strong absorption peak appeared at 340 nm and the peak at 400 nm is disappear (Fig. 1). The same tests were applied to other anions no obvious colour changes were observed for the receptor **4**. Absorbance ratio $(A-A_0)/A_0$ is displayed (Fig. 2). As can be seen from Fig. 1, it is clear that there was marked quenching upon addition of hydrogen sulfate, and no prominent change was observed upon addition of any F^- , Cl^- , Br^- , I^- , CH_3COO^- , H_2PO_4^- , NO_3^- and CN^- . The hydrogen bonding between O atom of HSO_4^- and the one NH moieties and Zn^{2+} ion of receptor **4** of the amide group dominates the overall H-bonding interaction. The ability of receptor **4** to recognised HSO_4^- in real environment was confirmed through competitive binding assay (Fig. 3). As shown in Fig. 3, no significant variation in the absorbance intensity is noticed by comparing the profile with and without the other anions, means that receptor **4** has a high selectivity for HSO_4^- even in the presence of other anions, suggesting that receptor **4** possesses an excellent selectivity for HSO_4^- over competitive anions.

Figure 4 shows the changes in the UV–vis spectrum of receptor **4** as a function of HSO_4^- concentration. The low-lying MLCT absorption and the high-energy $\pi-\pi^*$ ligand-based absorptions decrease monotonically during the addition, with saturation observed toward the end of the titration. A low-energy absorption feature concomitantly grows with increasing HSO_4^- concentration. These absorption features are likely a result of anion binding with the metal complex through the receptor **4**.

In the UV–vis titration of receptor **4**, the addition of increasing amounts of HSO_4^- ions (0 to 2 equiv) results in decrease in the absorption band at 400 nm and appearance

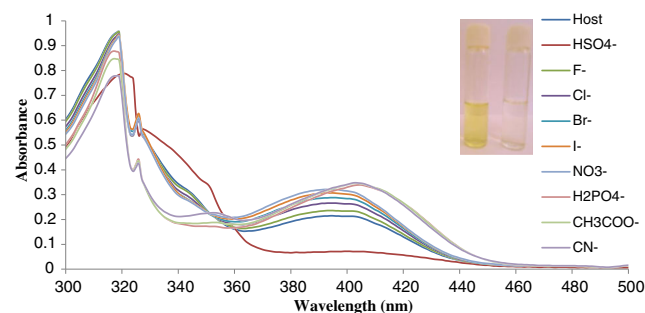


Fig. 1 Absorbance spectrum of receptor **4** (10 μM) upon the addition of fixed amount of anion (100 μM) in $\text{CH}_3\text{OH}:\text{H}_2\text{O}$ (70:30, v/v). The inset represents the colorimetric colour change from yellow green to colourless

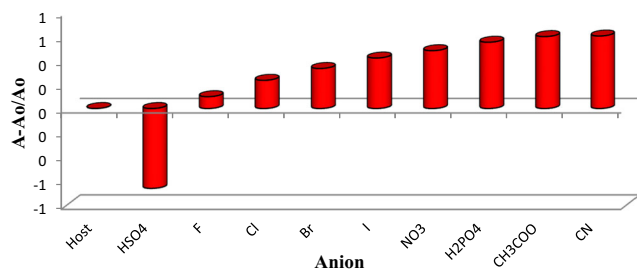


Fig. 2 Absorbance ratiometric response of receptor **4** (10 μM) upon the addition of a particular anions (100 μM) in $\text{CH}_3\text{OH}:\text{H}_2\text{O}$ (70:30, v/v)

of a new peak at 340 nm (Fig. 4). Furthermore, an isosbestic point at 358 nm was observed which indicates only one type of **4**. HSO_4^- complex formation and 1:1 stoichiometry of **4**. HSO_4^- complex (vide infra). A linear relationship was observed between concentrations of HSO_4^- with a high correlation coefficient. The inset of Fig. 4 represents a plot between normalized absorbance intensity versus concentrations of HSO_4^- in the $\text{CH}_3\text{OH}:\text{H}_2\text{O}$ (70:30, v/v) solution.

The emission profile of receptor **4** consists of band at 500 nm, upon excite at 400 nm (Fig. 5). The anion binding ability of receptor **4** was evaluated through addition of tetrabutylammonium salts of various anions (F^- , Cl^- , Br^- , I^- , CH_3COO^- , H_2PO_4^- , NO_3^- , CN^- and HSO_4^-) in $\text{CH}_3\text{OH}/\text{H}_2\text{O}$ (70:30, v/v) solvent system. It was notified that most of anion did not cause any significant change in emission spectrum of receptor **4** expect HSO_4^- . The addition of HSO_4^- leads to decrease as well as blue shift in fluorescence intensity of receptor **4**. The quenching of fluorescence may result from the electron repelling effect of HSO_4^- and partly from the change of ligand rigidity because of HSO_4^- binding. Both effects can discourage ligand to metal charge transfer (LMCT) and thus reduce fluorescence intensity.

Fig. 3 Interference of anions at the time of detection of HSO_4^- ion for receptor **4**

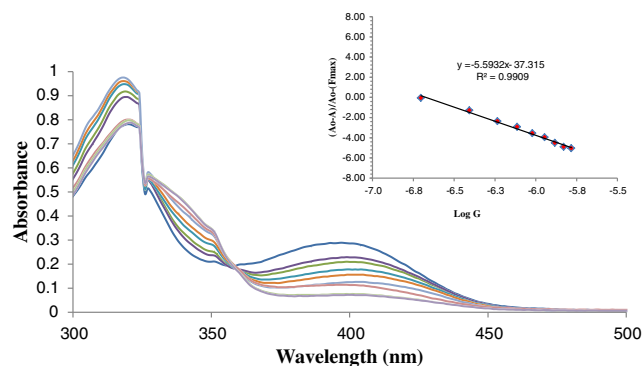
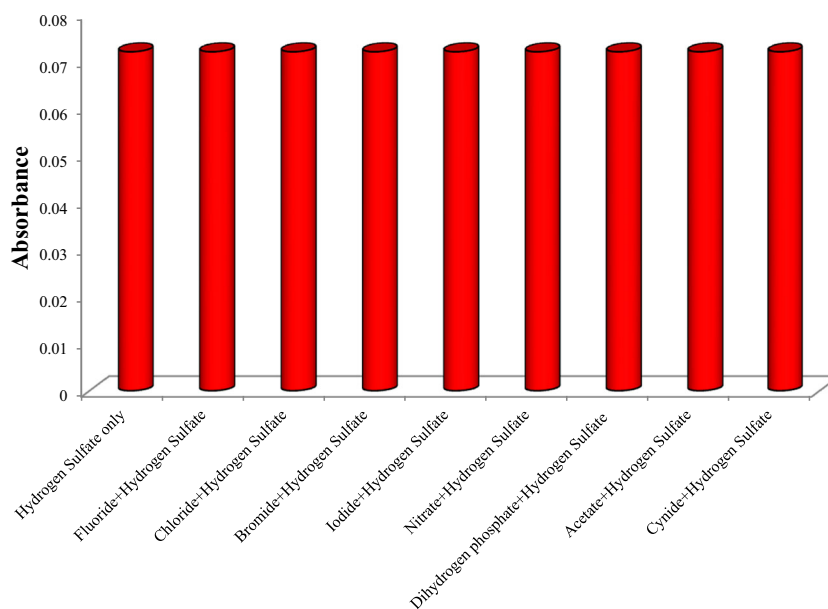


Fig. 4 Changes in absorbance spectrum of receptor **4** (10 μM) upon the gradually addition of HSO_4^- anion (100 μM) in $\text{CH}_3\text{OH}:\text{H}_2\text{O}$ (70:30, v/v). The inset represents the normalized response of absorbance signal with regression 0.981

The Fig. 6 presents quenching of the steady-state fluorescence spectrum of receptor **4** upon successive addition of HSO_4^- titration. The emission spectrum shows fluorescence quenching on increasing HSO_4^- concentration. The inset of Fig. 6 shows the normalized fluorescence intensity versus concentration of HSO_4^- and plot has linearity in the concentration range of 0.2–80 μM of HSO_4^- . The receptor **4** exhibited a high sensitivity toward HSO_4^- , 90 % quenching of its fluorescence intensity with 2 equiv of HSO_4^- . The expected explanation behind was turn ON PET due to donation of electron through O atom of HSO_4^- and internal charge transfer (ICT). Both the phenomena responsible to observable change on addition of HSO_4^- .

The binding stoichiometry of receptor **4**. HSO_4^- complexes was determined using Job's plot [14] experiments. In (Figure S1), the emission at 500 nm was plotted against the molar fraction of receptor **4** under a constant total concentration. A maximum emission was reached when the molar

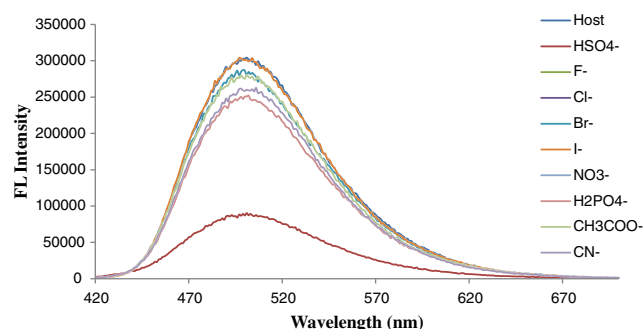


Fig. 5 Change in emission profile of receptor **4** (10 μM) upon the addition of different anion salt (100 μM) in $\text{CH}_3\text{OH}:\text{H}_2\text{O}$ (70:30, v/v)

fraction was 0.5. These results indicate a 1:1 ratio for both the receptor **4**: HSO_4^- complex. The association constant K_a was evaluated graphically by plotting $1/F - F_0$ against $1/G$ (Figure S2). The data was linearly fit according to the Benesi–Hilderbrand [15] equation and the K_a value was obtained from the slope and intercept of the line. The K_a values of receptor **4**: HSO_4^- complexes was $38,997 \text{ M}^{-1}$. The Stern–Volmer plot [16] (plot of F_0/F vs. concentration of guest) is a straight line shown in (Figure S3). This confirmed the formation of one type of complex between receptor **4** and HSO_4^- . Moreover, a minimum detection limit of 40 nM was achieved for HSO_4^- by receptor **4**, which was much lower than the maximum allowable our previous reported detection limit [17, 18].

All optimization studies were carried out by using B3LYP/631G basis set on Gaussian 09 program [19–21]. The receptor **3** has shown non-planar geometry in which two arms are totally opposite in direction. However, it showed drastic change in geometry on addition of Zn^{2+} , two arms come closer to each other and form an appropriate pseudocavity for Zn^{2+} as shown in Fig. 7. The various angles and dihedral angles are listed (Table 1), which represents the change in geometry on coordination with Zn^{2+} . A DFT optimized structure of complex **4** is also explained fluorescent nature of complex (Fig. 7). In complex **3**: Zn^{2+} , Zn atom in square pyramid environment which is consist of two Cl atoms (Cl48 and

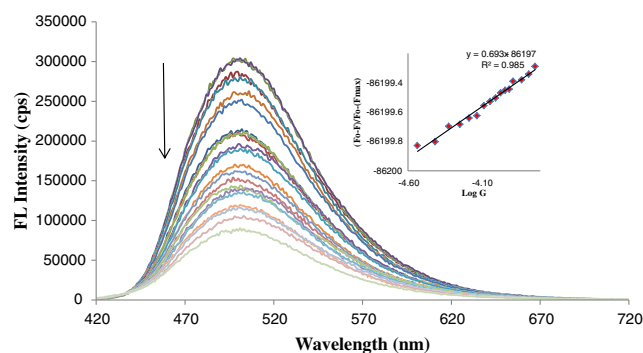


Fig. 6 Fluorescence titration of receptor **4** (10 μM) upon the addition of HSO_4^- salt (100 μM) in $\text{CH}_3\text{OH}:\text{H}_2\text{O}$ (70:30, v/v). The inset represents normalized response of fluorescence signal with 0.985 regressions

Cl49), two O atoms (O31 and O29) and N atom (N18). The additions of HSO_4^- result into replacement of Cl with O of HSO_4^- . Some of the selected bond parameters were compared and shown in Table 1.

In conclusion, our experimental results indicated that based on a tridentate binding model of Zn^{2+} complex of receptor **4**, is an attractive sensor for the fast detection of HSO_4^- in aqueous solution with exceptional selectivity. The sensor exhibited fluorescent shift in its emission spectra in response to HSO_4^- in aqueous solution, allowing hypersensitive HSO_4^- detection (detection limit up to 40 nM). The sensing has been suggested to proceed via a standing emission quenching process. The various studies (fluorescence, UV-Vis and DFT calculations) are suggestive of the formation of a hydrogen-bonded complex between the amide and sites of the receptor **4** and HSO_4^- there by supporting the standing quenching course of action.

Experimental

All commercial grade chemicals and solvents were used without further purification. The Fluorescence and UV-Visible spectra were recorded on Fluoromax-4 Spectrofluorometer and Shimadzu UV-24500 with 5 nm slit width and the chloride salt of metal used in study. Ultrapure water with a Millipore Purification System (Milli-Q water) was used throughout the analytical experiments. ^1H -NMR spectra were recorded on a Varian NMR mercury System 300 spectrometer operating at 300 MHz in CDCl_3 . The tetrabutyl ammonium salt of anions was used for studies.

Sample Preparation

A stock solution of probe **4** (1 mM) in $\text{CH}_3\text{OH}:\text{H}_2\text{O}$ (70:30, v/v) solution was prepared (receptor **4** is freely soluble in methanol at 25 $^\circ\text{C}$), and the corresponding working solutions (10 mM) were simply prepared by diluting with $\text{CH}_3\text{OH}:\text{H}_2\text{O}$ (70:30, v/v). All stock and working solution were prepared in ultrapure water and spectroscopic grade DMSO. Stock solution of anion (10 mM) was prepared with $\text{CH}_3\text{OH}:\text{H}_2\text{O}$ (70:30, v/v) solution and the corresponding working solutions (100 μM) were simply prepared by diluting with $\text{CH}_3\text{OH}:\text{H}_2\text{O}$ (70:30, v/v).

UV Visible Analysis

The UV-visible spectrophotometer experiments were carried out with Shimadzu UV-24500 spectrophotometer in $\text{CH}_3\text{OH}:\text{H}_2\text{O}$ (70:30, v/v) solvent system at room temperatures with the aim of determining the selectivity among the

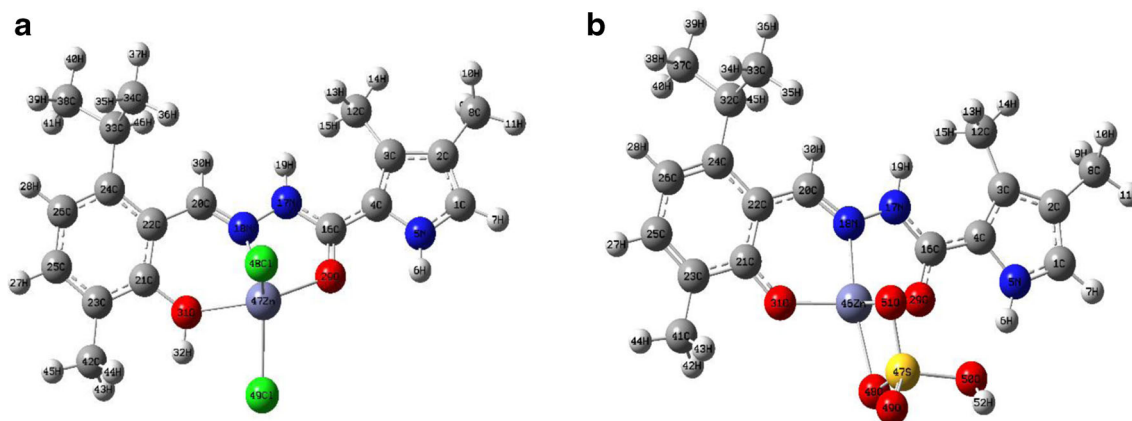


Fig. 7 The DFT optimized structure of: **a** 3.ZnCl₂ and **b** 4.HSO₄ calculated at the B3LYP/6-31G level. The red, blue, gray, dark gray, yellow and green spheres refer to O, N, C, Zn, S and Cl atoms respectively

anion (F⁻, Cl⁻, Br⁻, I⁻, CH₃COO⁻, HSO₄⁻, NO₃⁻ and CN⁻) in CH₃OH:H₂O (70:30, v/v) with receptor/ligand. The titration experiment was performed for showing satisfactory linear relationship between concentrations and absorbance intensity and for correlation coefficient. These titration experiments were accomplished through a stepwise addition of anion (100 μM) to a solution of receptor **4** (100 μM) in CH₃OH:H₂O (70:30, v/v) solution. The absorbance spectra were recorded in the range of 200–600 nm.

Fluorescence Analysis

The fluorescence titration experiments were carried out with a Fluoromax-4 spectrofluorometer in CH₃OH:H₂O (70:30, v/v) solvent system at room temperatures (298 K) with the aim of determining the association constant (K) for receptor/ligand

Table 1 Optimized bond angles, bond angles and energies calculated at the B3LYP/6-31G level

| Parameter | 3.Zn ²⁺ | 4.HSO ₄ ⁻ |
|-----------------|--------------------|---------------------------------|
| Bond angles (°) | | |
| C4–C16–N17 | 119.9 | 120.9 |
| N17–N18–C20 | 117.7 | 119.4 |
| C21–C22–N20 | 121.6 | 120.6 |
| C22–C20–N18 | 126.2 | 124.8 |
| N18–N17–C16 | 119.3 | 115.5 |
| O29–C16–N17 | 119.2 | 118.6 |
| Bond length (Å) | | |
| C21–O31 | 1.38 | 1.32 |
| C16–O29 | 1.27 | 1.28 |
| C16–N17 | 1.37 | 1.33 |
| N17–N18 | 1.38 | 1.39 |
| C4–C16 | 1.43 | 1.43 |
| Energy (a.u.) | -3713.8563 | -3492.1844 |

4-anion in this solvent system. These titration experiments were accomplished through a stepwise addition of HSO₄⁻ solutions (100 μM) to a solution of receptor **4** (10 μM) in CH₃OH:H₂O (70:30, v/v) solution. The fluorescence intensity was recorded at λ_{ex}/λ_{em} = 400/500 nm alongside a reagent blank. The excitation and emission slits were both set to 5.0 nm. After each addition enough time was given to attain the equilibrium. Then, the fluorescence data were collected and processed using the Benesi-Hildebrand Plot calculate the association constant (K) of the appropriate anion complexes.

Synthesis of Schiff Bases (3) of 3,4-Dimethyl-1H-Pyrrole-2-Carbohydrazide from Aromatic Aldehydes

The Schiff bases were prepared by reaction of equimolar quantities of 3,4-dimethyl-1H-pyrrole-2-carbohydrazide **2** and substituted aromatic aldehyde. Each reactant was dissolved in a minimum amount of ethanol, and then mixed together. The solution was refluxed for 3–4 h then cooled to room temperature and poured in to ice cold water. The obtained solid product was collected by filtration and then dried using drying oven at 70 °C. The product was re-dissolved in ethanol for recrystallization and then dried to give a pure product. A white powder, yield: 48 %; mp: 216–218 °C [22].

Synthesis of Receptor 4

Receptor **4** was synthesized by reaction of one mole of receptor **3** (0.314 g, 1 mmol) with one moles of ZnCl₂ (0.136 g, 1 mmol) in 50 ml MeOH stirring for 3 h at room temperature. The precipitation was collect by filtration at room temperature and dried in vacuum. Further it was washed with water then ethanol followed by petroleum ether [22].

References

1. Lehn JM (1995) Supramolecular chemistry—concept and perspective. VCH, Weinheim
2. Fegade U, Attarde S, Kuwar A (2013) Fluorescent recognition of Fe^{3+} ion with photoinduced electron transfer (PET) sensor. *Chem Phys Lett* 584:165–171
3. Fegade U, Sharma H, Bondhopadhyay B, Basu A, Attarde S, Singh N, Kuwar A (2014) “Turn-ON” fluorescent dipodal chemosensor for Nano-molar detection of Zn^{2+} : application in living cells imaging. *Talanta* 125:418–424
4. Fegade U, Sharma H, Attarde S, Singh N, Kuwar A (2014) Urea based dipodal fluorescence receptor for sensing of Fe^{3+} ion in semi-aqueous medium. *J Fluoresc* 24:27–37
5. Fegade U, Marek J, Patil R, Attarde S, Kuwar A (2014) A selective fluorescent receptor for the determination of nickel (II) in semi-aqueous media. *J Lumin* 146:234–238
6. Fegade U, Sharma H, Singh N, Ingle S, Attarde S, Kuwar A (2014) An amide based dipodal Zn^{2+} complex for multications recognition: nanomolar detection. *J Lumin* 149:190–195
7. Fegade U, Tayade S, Chaitanya GK, Attarde S (2014) A, kuwar, fluorescent and chromogenic receptor bearing amine and hydroxyl functionality for iron(III) detection in aqueous solution. *J Fluoresc* 24:675–681
8. Fegade U, Suban K (2014) Sahoo, Sanjay Attarde, Anil Kuwar, colorimetric and fluorescent “On-Off” chemosensor for Cu^{2+} in semi-aqueous medium. *Sensors Actuators B* 202:924–928
9. Cametti M, Rissanen K (2009) Recognition and sensing of fluoride anion. *Chem Commun* 20:2809–2829
10. Duke RM, Gunnlaugsson T (2011) 3-urea-1, 8-naphthalimides are good chemosensors: a highly selective dual colorimetric and fluorescent ICT based anion sensor for fluoride. *Tetrahedron Lett* 52: 1503–1505
11. Ebbesen P (1972) DEAE-dextran and polybrene cation enhancement and dextran sulfate anion inhibition of immune cytolysis. *J Immunol* 109:1296–1299
12. Kumar V, Kumar A, Diwan U, Upadhyay KK (2012) Uncovering the true mechanism of optical detection of HSO_4^- in water by Schiff-base receptors hydrolysis vs. Hydrogen Bonding. *Chem Commun* 48:9540–9544
13. Fegade U, Attarde S, Sahoo SK, Singh N, Kuwar A (2014) A selective and discriminating noncyclic receptor for HSO_4^- ion recognition: 2, 2-(pyridine-2,6-diylbis(azanediyl)) bis (methylene) diphenol. *RSC Adv* 4:15288–15292
14. Job P (1928) Formation and stability of inorganic complexes in solution. *Ann Chim* 9:113–203
15. Benesi HA, Hildebrand JH (1949) A spectrophotometric investigation on the interaction of iodine with aromatic hydrocarbons. *J Am Chem Soc* 71:2703–2707
16. Stern O, Volmer M (1919) About the decay of the fluorescence. *Phys J Phys Z* 20:183
17. Yang S-T, Liao D-J, Chen S-J, Hu C-H, Wu A-T (2012) A fluorescence enhancement-based sensor for hydrogen sulfate ion. *Analyst* 137:1553–1555
18. Li Q, Shao YGS (2012) A BODIPY derivative as a highly selective “Off-On” fluorescent chemosensor for hydrogen sulfate anion. *Analyst* 137:4497
19. Becke AD (1993) Density functional thermo chemistry. III. The role of exact exchange. *J Chem Phys* 98:5648–5652
20. Lee C, Yang W, Parr RG (1988) Development of the colle–salvetti correlation-energy formula into a functional of the electron density. *Phys Rev B* 37:785–789
21. Singh N, Kaur N, Mulrooney RC, Callan JF (2008) A ratiometric fluorescent probe for magnesium employing excited state intramolecular proton transfer. *Tetrahedron Lett* 49:6690–6692
22. Bhosale J, Fegade U, Bondhopadhyay B, Kaur S, Singh N, Basu A, Bendre R, Kuwar A, Pyrrole-coupled salicylimine-based fluorescence “turn on” probe for highly selective recognition of Zn^{2+} ions in mixed aqueous media: application in living cell imaging. *J Mol Recognit*. doi:10.1002/jmr.2451